

Energy Management for Joint Operation of CHP and PV Prosumers inside a Grid-connected Microgrid: A Game Theoretic Approach

Li Ma, Nian Liu, *Member, IEEE*, Jianhua Zhang, *Member, IEEE*, Wayes Tushar, *Member, IEEE*, and Chau Yuen, *Senior Member, IEEE*

Abstract—This paper mainly focuses on the energy management of microgrids (MGs) consist of combined heat and power (CHP) and photovoltaic (PV) prosumers. A multi-party energy management framework is proposed for joint operation of CHP and PV prosumers with the internal price-based demand response. In particular, an optimization model based on Stackelberg game is designed where the microgrid operator (MGO) acts as the leader and PV prosumers are the followers. The properties of the game are studied and it is proved that the game possesses a unique Stackelberg equilibrium. The heuristic algorithm based on differential evolution is proposed that can be adopted by the MGO, and nonlinear constrained programming can be adopted by each prosumer to reach the Stackelberg equilibrium. Finally, via a practical example, the effectiveness of the model is verified in terms of determining MGO's prices and optimizing net load characteristic, etc.

Index Terms—microgrid, combined heat and power, energy management, demand response, Stackelberg game.

I. INTRODUCTION

Due to increasing population growth and concerns for environmental pollution and climate change, the current power grid is facing the challenges of increasing demand, environmental protection, high reliability requirement, cleanness of energy and planning restrictions. As a potential solution to these concerns, centralized generating facilities are now being transformed into smaller and more distributed generations. However, indiscriminate usage of such distributed generation can also be detrimental for the power system. As a consequence, the concept of microgrid (MG) emerges. An MG can operate as a single controllable system and can be assumed as a cluster of loads and distributed energy

resources (DERs), which may include wind turbines (WTs), photovoltaics (PVs), fuel cells (FCs) and micro turbines (MTs), energy storage systems (EESs) and so on. In order to improve the operation efficiency, Energy Management System (EMS) is the essential part of the MGs.

From the perspective of modeling with involving resources in MGs, there are different considerations according to specific objects. For the renewable energy sources (RES) (such as WTs and PVs), the most important are maximal consumption of uncertainty produced power [1]. If the RESs are grid-connected system, the related Feed-in-Tariffs are also important for the operation. For the EESs, there is more attention paid on the designing of charging and discharging strategy. If the EESs are coordinated with the RESs, the strategy can be designed to assist the utilization of RESs, such as smooth the power fluctuation [2] and improve the self-consumption of renewable energy [3]. If the EESs are configured for demand response (DR), the strategy should be designed considering the price signal and load demand [1]. Moreover, the cycle life cost of batteries is also an important problem of the EESs [4]. For the fossil fueled DERs (such as diesel generation and microturbine), minimize the fuel cost of operation is the basic principle [5]. For Combined Heat and Power (CHP) system based on MTs or FCs, its outputs are not only the electric energy but also the thermal energy [6]. According to the priority, there are generally two types of operation strategy for CHPs: heat-led mode and electricity-led mode [7]. For the modeling of load, the electric appliances are usually categorized into two types: one for baseline load, which is fixed and cannot be scheduled; the other for shiftable load, which is flexible and can be treated as variables during the scheduling [8]. Therefore, in order to realize the optimal operation of MGs, the EMSs should be designed with the specified optimization models and algorithms, which mainly decided by the involving types of resources and the interaction among them.

From the perspective of optimization, there are mainly two types of methods: centralized optimization and distributed optimization. For the centralized optimization, there is only one operator in an MG. All the components inside the MG are supposed can be monitored by the operator, including all the DERs and loads [9, 10]. The decision variables may include controllable DERs and shiftable load. Generally, the objective of optimization is diversified by different purpose of MGs, such as minimize operation cost, carbon emission, loss of renewable energy, and so on [1, 11]. However, in a large scale

Manuscript received December 1, 2015; revised March 2, 2016 and May 4, 2016; accepted May 29, 2016. This work was supported in part by the National Natural Science Foundation of China under grant 51277067, in part by the National High-tech R&D Program of China (863 Program) under grant 2014AA052001, and in part by the Fundamental Research Funds for the Central Universities under grant 2015ZD02. The work of C. Yuen and W. Tushar was supported by Grant NRF2015ENC-GBICRD001-028. Paper no. TII-15-1786.

L. Ma, N. Liu and J. Zhang are with State Key Laboratory of Alternate Electrical Power System with Renewable Energy Sources, North China Electric Power University, Beijing 102206, China (e-mail: nian_liu@163.com).

L. Ma is also with the China Electric Power Research Institute, Beijing 100192, China.

W. Tushar and C. Yuen are with the Singapore University of Technology and Design (SUTD), Dover Drive, Singapore 138682.

system, the total number of constraints and decision variables can be very large. That means the computation requirement of the centralized optimization could be a problem. Moreover, with the development of Smart Grid, the researchers gradually find out that the operator may be not unique in an MG. The most typical case is that the loads belong to different users inside the MG, the operator could not have the privilege to monitor and control the users' appliances due to the autonomous and privacy constraints [12]. Similarly, the DERs may also be operated by different proprietors. So there are possibly a number of autonomous DER operators. Therefore, the centralized optimization is not suitable for the multi-party scenarios. Recently, in order to solve the problem, there are several types of distributed optimization methods are applied in MGs, which includes Game Theory-based distributed optimization [13], distributed convex optimization [14], and alternating direction method of multipliers [15], etc. Among them, Game Theory is a formal analytical as well as conceptual framework with a set of mathematical tools enabling the study of complex interactions among independent rational players [13].

In this paper, we focus on one type of hybrid multi-party MGs consist of CHP and PV prosumers, which we think it will have great application potential. On the one hand, considering the heating of many countries is rigid demand for residential buildings, the application of CHP system can provide the thermal and electrical energy for loads simultaneously with much higher efficiency [16]. On the other hand, with the encourage of energy policy, the distributed PV systems are developing very fast in residential communities. The MG is a suitable technique to improve local consumption of the PV energy and reduce the negative impact on the utility grid. For this type of MGs, the studies on the energy management are still limited. In [10], an EMS is designed for the MG including PV, ESS, and CHP. In [11], the multi-objective optimization was used to design EMS for an MG consist of CHP, WT, PV, thermal and electrical storage. In addition, DR is further considered in the optimization model, which is treated as virtual generation units [17]. In [18], a nonlinear optimal model was proposed for economic operation of the MG consists of CHP, WT, PV and ESS, which also considers the effect of ESS and peak-valley electricity price. As can be seen from these studies, the EMS is designed based on centralized optimization, which assumes all the DERs and loads can be monitored and controlled. However, the multiple independent parties inside an MG are a disturbance for the application of centralized optimization. The reasons are mainly on two aspects: 1) as the PV prosumers are highly independent and autonomous, the MG operator (MGO) cannot access their detail information for privacy concern; 2) the MGO cannot make decisions or schedules for the prosumers, since the individual needs of prosumers have led to differences in their decision-making.

We stress that recent work has shown Stackelberg games to be very effective and suitable for designing distributed energy management schemes in Smart Grid, especially for the electricity-trading process between the service provider and users [19, 20]. For the hybrid multi-party MGs consist of CHP and PV prosumers, the relationship between MGO and PV prosumers is just a bi-directional trading process. If the PV

energy is not sufficient, the prosumer would buy electricity from the MGO. Otherwise, the prosumer would sell electricity to the MGO. In this regard, the distributed optimization can be achieved with the electricity-trading process between MGO and PV prosumers by using Stackelberg game. However, other aforementioned distributed optimization methods may solve the problem differently without the trading process, which also mean that the energy management may have difficulties on applications. Thus, we think it is more suitable to model the distributed energy management of the hybrid MG by using Stackelberg game.

To this end, this paper will focus on distributed energy management for the smart MG with heat-led CHP and PV prosumers by making the following contributions:

- 1) An energy management framework for joint operation of heat-led CHP and PV prosumers inside the grid-connected MG are introduced, considering the interactions between MGO and prosumers with automatic demand response (ADR) ability.
- 2) An optimization model for jointly operating the MG is proposed. The model is designed based on Stackelberg game, where the MGO acts as the leader and all participating prosumers are considered as the followers.
- 3) The properties of the game are studied and it is shown that there exists a unique Stackelberg equilibrium. The best strategies of MGOs prices and corresponding shiftable arrangements for prosumers are determined with this Stackelberg equilibrium.
- 4) The differential evolution-based heuristic algorithm and nonlinear constrained programming are adopted by the MGO and each prosumer respectively to reach the Stackelberg equilibrium.

II. ENERGY MANAGEMENT FRAMEWORK

A. System architecture and functions

The system architecture of the MG is shown in Fig. 1. Each prosumer in the MG is comprised of user energy management system (UEMS), PV source, load, smart meters, and so on. The MGO also has its own sources, such as microturbines, and it could be affiliated with an electric power seller [17]. At the same time, the MGO is the EMS executor of MG, and mandatory to assure the interoperability among various components in Fig. 1. The MGO is in charge of providing heat output to all the prosumers in the MG. It also possesses the function of purchasing electricity from the utility grid or from the prosumers with surplus RES power output, and then selling electricity to users within the MG. Furthermore, the MGO also guarantees the maximum utilization of PVs within the MG system.

For any prosumer in the MG, PV source is the first choice of electric power, and it will purchase electricity provided by the MGO when PV source can not satisfy the load demands. On the other hand, if demands of the prosumer is less than the production of PV source, the redundant PV power outputs will be sold to the MGO, who will sell them to the other prosumers in the MG or sell them back to the utility grid with different prices.

The UEMS of the prosumer is utilized to gather data of PV source, electric load and heat load, and receive instructions or

information from the MGO. In addition, it is in charge of control and optimization of the appliance energy consumption of prosumers. Due to the intermittent nature of PV production, a forecasting function should also be added to the UEMS to provide power output predictions of the installed PVs.

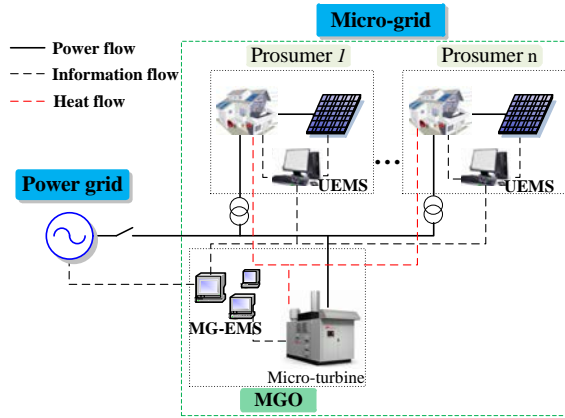


Fig. 1. System architecture of the MG

B. Operating strategy

The microturbine is operated with heat-led operation strategy, which is defined as operation in an attempt to meet, but not exceed, the onsite heat demand using the direct thermal output from the prime mover technology [7]. Heat demand is subject to technical constraints, and if necessary can be exceeded via delivery of excess to the thermal energy storage system or the small allowable heat dump. The influence relationships of the power grid, MGO and UEMS are shown in Fig. 2.

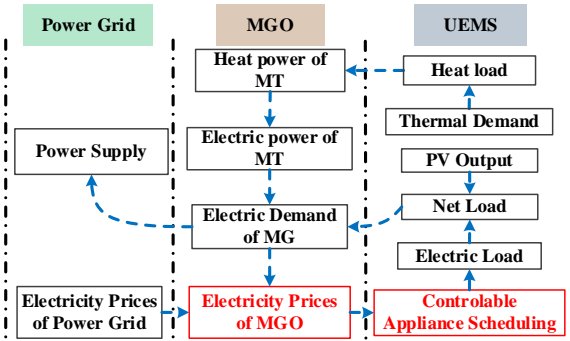


Fig. 2. Schematic diagram of influence relationships.

As shown in Fig. 2, the UEMS of a prosumer determines the heat load based on the prosumer's thermal demand. It also receives the selling and buying prices from the MGO, and optimizes its energy consumption of controllable appliances according to these price information. Considering the PV power output and other uncontrolled appliances' energy consumption, the UEMS can figure out the prosumer's net load and send it to the MGO.

For a MGO, it receives the heat load demand from all the prosumers, and the microturbine will produce heat power equivalent to this value. The microturbine also produces electric power at the same time. Taking into account all prosumers' net loads and the electric power of the microturbine, MGO can calculate the power demand of the whole MG, and send the information to the power grid. On the other hand, the prosumers' redundant PV outputs are also sold to the MGO. If the sum of these PV outputs and microturbine's

electric power exceed the load demand of the MG, the MGO will sell them back to the power grid.

The power grid will supply the electricity to the MG, and buy the redundant electricity from the MG when needed. It also sends its price information to the MGO. The MGO will optimize the selling and buying prices according to the power grid prices as well as the electric demand of the MG, which depends on the energy consumption of prosumers' controllable appliances.

III. BASIC MODEL OF MG

A. Model of PV prosumers

1) Electric load requirements

All prosumers participating in the DR are supposed to have a certain proportion of flexible load, which means they have the room for adjusting the size and time of the load. In this study, prosumers' load is comprised of two types, i.e., fixed load and shiftable load. In addition, the power output of PV will also offset the load of the prosumer.

a) Fixed load

Fixed load requires high reliability and the time of power supply is immutable. So the fixed load has no contribution to DR and it is necessary to guarantee the power supply for fixed load first. In this paper, the loads such as lights, televisions, refrigerators, elevators, etc. are considered as fixed loads for ensuring the daily-life convenience. The fixed load set of prosumer i in the specified time period is defined as:

$$\mathbf{fl}_i \triangleq [fl_i^1, fl_i^2, \dots, fl_i^H], \quad i \in [1, 2, \dots, n] \quad (1)$$

where n is the total number of prosumers in the MG, and H is the length of time horizon, which is 24 hours in this study.

b) Shiftable load

Shiftable load means that consumers can choose the time when they use the electricity according to the electricity price. In this paper, each prosumer is assumed to have dozens or hundreds of shiftable load appliances or equipments. Such appliances or equipments may include PHEVs, washers, dryers, dishwashers, etc. The shiftable load set of prosumer i in the specified period is defined as:

$$\mathbf{sl}_i \triangleq [sl_i^1, sl_i^2, \dots, sl_i^H], \quad i \in [1, 2, \dots, n] \quad (2)$$

Assuming the number of the shiftable loads of prosumer i is K_i , the shiftable load value of prosumer i at period h is the sum of all its shiftable loads:

$$sl_i^h = \sum_{k=1}^{K_i} sl_{ik}^h \quad (3)$$

where sl_{ik}^h is the shiftable load k of prosumer i at period h . The detailed model of shiftable load involves the size, total amount, duration time and optional time range of the load. The specific expression is as follows:

$$\begin{cases} sl_{ik}^h \in [sl_{ik}^{\min}, sl_{ik}^{\max}], & h \in [t_{ik}, t_{ik} + \Delta T_{ik}] \\ sl_{ik}^h = 0, & h \notin [t_{ik}, t_{ik} + \Delta T_{ik}] \end{cases} \quad (4)$$

$$[t_{ik}, t_{ik} + \Delta T_{ik}] \in [\alpha_{ik}, \beta_{ik}] \quad (5)$$

$$\sum_{h=t_{ik}}^{t_{ik} + \Delta T_{ik}} sl_{ik}^h = sq_{ik} \quad (6)$$

In these equations, $[sl_{ik}^{\min}, sl_{ik}^{\max}]$ is the range of the electric power of shiftable load k for prosumer i , t_{ik} is the start time of the shiftable load k , ΔT_{ik} is the duration time of the shiftable load k , $[\alpha_{ik}, \beta_{ik}]$ is the optional time range interval of the shiftable load k , and sq_{ik} is the demand amount of the shiftable load k , which is the sum of all power consumption of

every period. In addition, t_{ik} and $t_{ik} + \Delta T_{ik}$ need to be within the time range $[\alpha_i, \beta_i]$.

In order to simplify the subsequent calculation, we simplify the model of sl_i^h , which involves the size, total amount and optional time range of the load:

$$\begin{cases} sl_i^{\min} < sl_i^h < sl_i^{\max}, & h \in [\alpha_i, \beta_i] \\ sl_i^h = 0, & h \notin [\alpha_i, \beta_i] \end{cases} \quad (7)$$

$$\sum_{h=1}^H sl_i^h = sq_i \quad (8)$$

In these representations, sl_i^h is regarded as a continuous variable, $[sl_i^{\min}, sl_i^{\max}]$ is the range of sl_i^h , which can be determined by the monte carlo method according to equations (3)~(6), $[\alpha_i, \beta_i]$ is the optional time range interval of the shiftable load, and sq_i is the demand amount of the shiftable load, which is the sum of shiftable loads of all periods.

In subsequent sections, when $[sl_i^1, sl_i^2, \dots, sl_i^H]$ is solved, we can determine the start time of each shiftable load in turn, which will be introduced later.

2) Heat load requirements

The heat produced by CHPs would be used to satisfy the thermal demand of the prosumers. Thermal demand of a user often consists of hot water or low pressure steam demand in the winter and a cooling demand in the summer. Heat from the prime movers often used in a single-stage steam or hot water absorption chiller. This option allows the CHP system to operate continuously throughout the year while maintaining a good thermal load without rejecting heat to the environment. The thermal demand, i.e., the heat load set of prosumer i in the specified period is defined as:

$$\mathbf{hl}_i \triangleq [hl_i^1, hl_i^2, \dots, hl_i^H], \quad i \in [1, 2, \dots, n] \quad (9)$$

3) Output power of PV

The output power of a PV cell changes with solar intensity and environment temperature, but there is only one maximum power point (MPP) for a specified situation. A PV system usually uses the maximum power point tracking (MPPT) to make PV modules work at MPP in a varying environment. The predicted value of the PV source's active power of prosumer i in the specified period is defined as:

$$\mathbf{pv}_i \triangleq [pv_i^1, pv_i^2, \dots, pv_i^H], \quad i \in [1, 2, \dots, n] \quad (10)$$

B. Model of Microturbine

It is worth noting that a niche market has appeared for microturbine generators (MTGs) with output power of 20-500 kW. The model of microturbine consists of two parts, i.e., heat power and electric power.

1) Heat power

$$hp_{chp}^h = \sum_{i=1}^n hl_i^h \quad (11)$$

where hp_{chp}^h is the total heat load at period h , and hl_i^h is the heat load of prosumer i at period h .

2) Electric power[21]

$$hp_{chp}^h = \frac{ep_{chp}^h}{\eta_{chp}} \cdot (1 - \eta_{chp} - \eta_{loss}) \cdot \delta_{heat} \quad (12)$$

$$ep_{chp}^h = \frac{hp_{chp}^h}{\theta} \quad (13)$$

$$\theta = \frac{(1 - \eta_{chp} - \eta_{loss}) \delta_{heat}}{\eta_{chp}} \quad (14)$$

where ep_{chp}^h is the total electric load at period h ; η_{chp} is the power generation efficiency of the microturbine generator;

η_{loss} is the heat loss coefficient; so $\frac{ep_{chp}^h}{\eta_{chp}} \cdot (1 - \eta_{chp} - \eta_{loss})$ is the waste heat of the microturbine generator; δ_{heat} is the heating coefficient. The relation between ep_{chp}^h and hp_{chp}^h can be expressed as equation (13), where θ is the heat-to-electric ratio defined as equation (14).

C. Model of MG system

According to the models of fixed load, shiftable load and PV output, the net load of prosumer i at period h is defined as:

$$NL_i^h = tl_i^h - pv_i^h, \quad i \in [1, 2, \dots, n], h \in [1, 2, \dots, H] \quad (15)$$

$$\mathbf{NL}_i \triangleq [NL_i^1, NL_i^2, \dots, NL_i^H] \quad (16)$$

$$tl_i^h = fl_i^h + sl_i^h \quad (17)$$

Considering the MG as a system, the total net load of this system (denoted as system net load) at period h is the sum of all prosumers' net load:

$$NL^h = \sum_{i=1}^n NL_i^h \quad (18)$$

IV. ECONOMIC MODEL FOR OPERATION OF MG

A. Price model of power grid

One of the most common demand side management programs consists of time-of-use (TOU) prices, where consumers are charged differently depending on the time of the day when they make use of energy services. For example, a non-residential TOU prices have been implemented in Beijing. In this study, the TOU price model will be applied by the power grid. The prices provided by power grid are defined as:

$$\mathbf{p}_{gs} \triangleq [p_{gs}^1, p_{gs}^2, \dots, p_{gs}^H] \quad (19)$$

$$\mathbf{p}_{gb} \triangleq [p_{gb}^1, p_{gb}^2, \dots, p_{gb}^H] \quad (20)$$

where \mathbf{p}_{gs} is the selling price of the power grid, and \mathbf{p}_{gb} is the buying price, which is a constant within a day.

B. Profit model of the MGO

The prices provided by the MGO to the prosumers are defined as:

$$\mathbf{p}_{ms} \triangleq [p_{ms}^1, p_{ms}^2, \dots, p_{ms}^H] \quad (21)$$

$$\mathbf{p}_{mb} \triangleq [p_{mb}^1, p_{mb}^2, \dots, p_{mb}^H] \quad (22)$$

where \mathbf{p}_{ms} is the selling price to the prosumers, and \mathbf{p}_{mb} is the buying price from the prosumers, both of them are determined by the MGO, and

$$p_{ms}^h < p_{ms}^h, \quad h \in [1, 2, \dots, H] \quad (23)$$

$$(p_{mb}^h, p_{ms}^h) \in [p_{gb}^h, p_{gs}^h]. \quad (24)$$

The MGO gets profits from electricity trading and heat trading. The electricity amount of the MGO consists of three parts, i.e., the electricity from the power grid, from prosumers with surplus RES power output and from microturbine, which is owned by the MGO itself. Accordingly, the MGO's profit can be represented as follows:

$$Pro_M^h = Pro_{M,g}^h + Pro_{M,u}^h + Pro_{M,heat}^h - C_{CHP}^h \quad (25)$$

$$Pro_{M,g}^h = -p_{gs}^h \cdot \max(NL^h - ep_{chp}^h, 0) - p_{gb}^h \cdot \min(NL^h - ep_{chp}^h, 0) \quad (26)$$

$$Pro_{M,u}^h = \sum_{i=1}^n p_{ms}^h \cdot \max(NL_i^h, 0) + \sum_{i=1}^n p_{mb}^h \cdot \min(NL_i^h, 0) \quad (27)$$

$$Pro_{M,heat}^h = \gamma \cdot \sum_{i=1}^n hl_i^h \quad (28)$$

$$Pro_M = \sum_{h=1}^H Pro_M^h \quad (29)$$

where $Pro_{M,g}^h$ and $Pro_{M,u}^h$ are the profits of the MGO from the electricity trading with the power grid, prosumers in the MG, respectively; $Pro_{M,heat}^h$ is the profit that the MGO gains from providing heat power to the prosumers; γ is the price of

the heat power provided by the MGO; C_{CHP}^h is the cost of microturbine [21], which is defined as:

$$C_{CHP}^h = \left(p_{gas} / L \right) \cdot \left(hp_{chp}^h / \theta \cdot \eta_{chp} \right) \quad (30)$$

where p_{gas} is the price of natural gas; L is the low heating value of natural gas.

C. Profit model of individual prosumer

The profit of an individual prosumer consists of its utility, income of selling electricity, expenditure of buying electricity and heat, and subsidy of distributed PV generation from the government. It could be defined as:

$$Pro_{U_i}^h = k_i \cdot \ln(1 + tl_i^h) - p_{ms}^h \cdot \max(NL_i^h, 0) - p_{mb}^h \cdot \min(NL_i^h, 0) - hl_i^h \cdot \gamma + pv_i^h \cdot \alpha \quad (31)$$

$$Pro_{U_i} = \sum_{h=1}^H Pro_{U_i}^h \quad (32)$$

where α is the unit subsidy of distributed PV generation per kWh; $k_i \cdot \ln(1 + tl_i^h)$ is the utility that the prosumer i achieves from consuming electric power tl_i^h , and k_i is a preference parameter [19]. The profit of prosumer i with different k_i are shown in Fig. 3. The reason we choose $k_i \cdot \ln(1 + tl_i^h)$ as the utility function for prosumer is that the logarithmic function has been widely used in economics for modeling the preference ordering of users, and it is also closely related to the utility function that leads to proportionally fair demand response [19]. Moreover, we adopt $\ln(1 + tl_i^h)$ to avoid the singular point due to the divergence of $\ln(tl_i^h)$ when $tl_i^h = 0$.

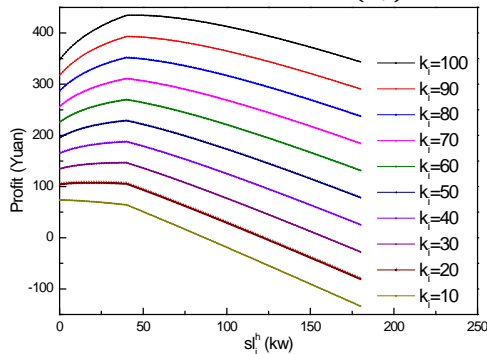


Fig. 3. Plot of prosumer's profit with different k_i . The other parameters in (31), i.e., fl_i^h , pv_i^h , hl_i^h , p_{ms}^h , p_{mb}^h , and γ are fixed as 20 kW, 60 kW, 20 kW, 1.5 Yuan, 0.5 Yuan and 0.1 Yuan respectively.

As shown in Fig. 3, the prosumer with higher k_i would attain more profit, and the prosumer's profit is a piecewise function with a cut-off point, where $NL_i^h = 0$, i.e., at $sl_i^h = 40$ kW. On the left side of the cut-off point, the curve with smaller k_i will possibly have a peak value higher than the cut-off point. While on the right side of the cut-off point, the curve with larger k_i will possibly have a peak value.

V. STACKELBERG GAME MODEL AND ALGORITHMS

A. Stackelberg game theory for the CHP-MG

In this paper, the trading problem within the MG is modeled as a non-cooperative Stackelberg game, where the MGO is the leader, and prosumers are the followers, to capture the interaction between the MGO and the prosumers. The objective of the MGO is to strategically choose the selling and buying prices that it offers to the prosumers so as to optimize a

utility that captures the tradeoff between the profit from selling electricity and heat power to the prosumers and the cost stems from the operation of microturbines. Based on the strategy chosen by the leader, each prosumer decides on the energy and heat amount that it buys from the MGO. Now, the Stackelberg game to capture this interaction between the MGO and the prosumers can be formally defined by its strategic form as:

$$G_{CM} = \{(\mathcal{N} \cup \{MGO\}); \mathbf{SL}_1, \dots, \mathbf{SL}_n; Pro_{U_i}, \dots, Pro_{U_n}; \mathbf{p}_{mb}; \mathbf{p}_{ms}; Pro_M\} \quad (33)$$

which consists of the following components:

i) The prosumers in set \mathcal{N} act as followers and choose their strategies in response to the prices set by the MGO, i.e., the leader of the game.

ii) $\{\mathbf{SL}_1, \dots, \mathbf{SL}_n\}$ is the set of strategies of each prosumer in \mathcal{N} from which it selects its strategy, i.e., $(\mathbf{sl}_1, \dots, \mathbf{sl}_n)$.

iii) $\{Pro_{U_i}, \dots, Pro_{U_n}\}$ is the profit function of each prosumer as explained in (31).

iv) \mathbf{p}_{mb} and \mathbf{p}_{ms} are the prices set by the MGO to buy and sell energy from/to the prosumers respectively.

v) The profit function Pro_M of the MGO as explained in (25) captures the total profit incurred by the MGO for trading energy with prosumers and the power grid.

Obviously, the objectives of each prosumer and the MGO are to maximize the profits in (31) and (25) respectively by their chosen strategies. For this purpose, one suitable solution for the proposed game in (33) is the Stackelberg equilibrium (SE) at which the leader obtains the optimal prices given the followers' best responses. At this equilibrium, neither the leader nor any follower can benefit, in terms of profits, by unilaterally changing their strategy [19].

A Stackelberg equilibrium, is a set of strategies, one for each player, such that no player has incentive to unilaterally change his/her action. G_{CM} 's Stackelberg Equilibrium is defined as follows:

Definition:

In the game defined as (33), a strategy set $(\mathbf{sl}_1^*, \dots, \mathbf{sl}_n^*, \mathbf{p}_{mb}^*, \mathbf{p}_{ms}^*)$ is a combination of the strategies from every player, i.e., MGO and the prosumers. For a random prosumer i , if its strategy \mathbf{sl}_i^* is the best strategy to the strategy combination $(\mathbf{sl}^*, \mathbf{p}_{mb}^*, \mathbf{p}_{ms}^*)$ of other players, i.e.,

$$Pro_{U_i}(\mathbf{sl}_i^*, \mathbf{p}_{mb}^*, \mathbf{p}_{ms}^*) \geq Pro_{U_i}(\mathbf{sl}_{-i}, \mathbf{sl}_i, \mathbf{p}_{mb}^*, \mathbf{p}_{ms}^*) \quad (34)$$

is correct for every random \mathbf{sl}_i , and

$$Pro_M(\mathbf{sl}^*, \mathbf{p}_{mb}^*, \mathbf{p}_{ms}^*) \geq Pro_M(\mathbf{sl}^*, \mathbf{p}_{mb}, \mathbf{p}_{ms}^*), \quad (35)$$

$$Pro_M(\mathbf{sl}^*, \mathbf{p}_{mb}^*, \mathbf{p}_{ms}^*) \geq Pro_M(\mathbf{sl}^*, \mathbf{p}_{mb}^*, \mathbf{p}_{ms}), \quad (36)$$

where $\mathbf{sl}^* = (\mathbf{sl}_1^*, \dots, \mathbf{sl}_n^*)$, $\mathbf{sl}_{-i}^* = (\mathbf{sl}_1^*, \dots, \mathbf{sl}_{i-1}^*, \mathbf{sl}_{i+1}^*, \dots, \mathbf{sl}_n^*)$, then the strategy set $(\mathbf{sl}^*, \mathbf{p}_{mb}^*, \mathbf{p}_{ms}^*)$ is termed as a 'Stackelberg Equilibrium' of G_{CM} .

For the proposed G_{CM} , we need to further proof the existence and uniqueness of the Stackelberg equilibrium.

Theorem:

In the proposed Stackelberg game G_{CM} , a unique Stackelberg Equilibrium exists if the following conditions are satisfied [20].

1) The strategy set of each player is nonempty, convex, and compact.

2) Each prosumer has a unique optimal best-response strategy once informed of the MGO's strategy.

3) The MGO admits a unique optimal strategy given the identified best strategies of all the prosumers.

Proof 1): Because the sets $\{\mathbf{SL}_1, \dots, \mathbf{SL}_n\}$ and $\{\mathbf{P}_{mb}, \mathbf{P}_{ms}\}$ defined in the paper are sets of linear equality, i.e., constraint (8), and convex constraints, i.e., (7) and (23). These sets are readily defined as nonempty, convex, and compact [22].

The *Proof 2*) and *Proof 3*) are given in Appendix A and Appendix B, respectively.

In conclusion, a unique Stackelberg Equilibrium exists in the proposed Stackelberg game G_{CM} .

B. Algorithm to reach the Stackelberg Equilibrium

Obviously, it is unrealistic to connect all the prosumers' appliances directly to the MGO. An alternative is utilizing the decentralized optimization and control of prosumers, which is one of the main functions in UEMS. The implementation process of the Stackelberg game model needs collaborations between the UEMS and MGO, and is essentially a problem of Nonlinear Programming. It is difficult to directly obtain the optimal solution with conventional mathematical methods. Hence a heuristic optimization algorithm will be adapted to solve this problem. The differential evolution (DE) algorithm, proposed by Storn and Price [23], is an efficient and effective global optimizer. It has been successfully applied in various fields, and it is also applicable to solve the Stackelberg game problem in this paper. The fundamental of the algorithm is to randomly generate an initial population at first, then calculate iteratively with mutation, crossover and selection operations according to a certain principle. It will guide the search process to approach the optimal solution with the evolution of individual fitness. The general implementation process of the model executed by the MGO is shown in **Algorithm 1**.

Algorithm 1 Executed by the MGO.

- 1: Set parameters: $\mathbf{p}_{gs}, \mathbf{p}_{gb}, \gamma, \theta, p_{gas}, L, \eta_{chp}$ and $K = 0$.
 - 2: Randomly generate MGO prices, i.e., \mathbf{p}_{mb_1} and \mathbf{p}_{ms_1} .
 - 3: **Repeat**:
 - 4: $\mathbf{K}=\mathbf{K}+1$.
 - 5: **For** Each prosumer $i \in \mathcal{N}$ **Do**
 Send MGO prices and γ to prosumer $i \in \mathcal{N}$.
 Prosumer i Execute **Algorithm 2**.
 Receive the optimized net load and heat load of prosumer i .
 - 6: **End For**
 - 7: Calculate Pro_{M_K} based on equation (25).
 - 8: Perform mutation, crossover operations, generate offspring MGO prices $\mathbf{p}_{mb_K'}$ and $\mathbf{p}_{ms_K'}$.
 - 9: Execute step 4 ~ step 8 using offspring MGO prices, and Calculate $Pro_{M_K'}$ based on equation (25).
 - 10: **If** $Pro_{M_K'} > Pro_{M_K}$
 $\mathbf{p}_{mb_K+1} = \mathbf{p}_{mb_K'}, \mathbf{p}_{ms_K+1} = \mathbf{p}_{ms_K'}$
Else
 $\mathbf{p}_{mb_K+1} = \mathbf{p}_{mb_K}, \mathbf{p}_{ms_K+1} = \mathbf{p}_{ms_K}$
 - 11: **End If**
 - 12: **Until** iterative condition is satisfied.
-

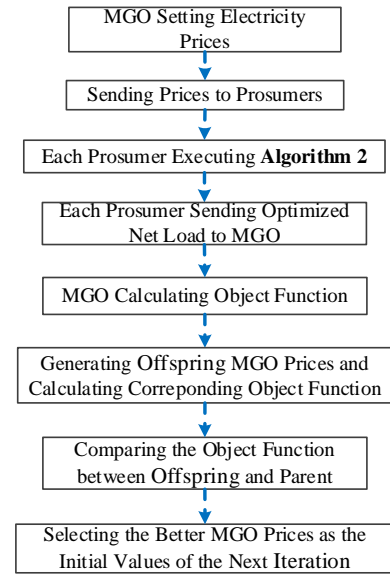


Fig. 4. The brief process in each iteration of **Algorithm 1**.

Algorithm 1 is executed by the MGO, and the optimizing variables are buying and selling prices provided for the prosumers. The object function is calculated based on each prosumer's optimized net load, which is determined by executing **Algorithm 2**, which is based on a nonlinear constrained programming method. This brief process in each iteration ($\mathbf{K} \geq 1$) of **Algorithm 1** is shown in Fig.4. The steps 8~11 in **Algorithm 1** correspond to the last three boxes in Fig.4.

Algorithm 2 Executed by prosumer i .

- 1: Set parameters: k_i, α .
 - 2: Receive $\mathbf{p}_{mb}, \mathbf{p}_{ms}$ and γ from the MGO.
 - 3: Optimize \mathbf{sl}_i by solving the following nonlinear constrained programming:

$$\max Pro_{U_i}$$

$$\text{s. t.}$$

$$sl_i^{\min} < sl_i^h < sl_i^{\max}, h \in [\alpha_i, \beta_i]$$

$$sl_i^h = 0, h \notin [\alpha_i, \beta_i]$$

$$\sum_{h=1}^H sl_i^h = sq_i$$
 The objective function, i.e., Pro_{U_i} can be calculated based on equation(31) and (32).
 - 4: Calculate the net load \mathbf{NL}_i based on the optimized \mathbf{sl}_i , the fixed load \mathbf{fl}_i and \mathbf{PV}_i , and send the optimized net load \mathbf{NL}_i to the MGO.
-

When **Algorithm 1** has been finished, the MGO sends the final optimized \mathbf{sl}_i (denoted as \mathbf{sl}_{i_opt} , $\mathbf{sl}_{i_opt} \triangleq [sl_{i_opt}^1, sl_{i_opt}^2, \dots, sl_{i_opt}^H]$) to prosumer $i, i \in [1, 2, \dots, n]$. Then **Algorithm 3** is executed by each prosumer to determine the start times of all shiftable loads. The principle of **Algorithm 3** is that the shiftable load determined by these start times (denoted as \mathbf{sl}_{i_adj} , $\mathbf{sl}_{i_adj} \triangleq [sl_{i_adj}^1, sl_{i_adj}^2, \dots, sl_{i_adj}^H]$) is close to \mathbf{sl}_{i_opt} as much as possible. For the sake of simplicity, it's assumed that $sl_{ik}^{\min} = sl_{ik}^{\max} = sl_{ik}$ in equation (4). Then $sl_{i_adj}^h$ can be expressed as:

$$sl_{i_adj}^h = \sum_{k=1}^{K_i} \text{sign}\{\max[(h - t_{ik} + 1) * (t_{ik} + \Delta T_{ik} - h)], 0\} * sl_{ik} \quad (37)$$

Algorithm3 Executed by prosumer i .

- 1: Receive sl_{i_opt} from the MGO.
- 2: Optimize t_{ik} ($k \in [1, 2, \dots, K_i]$) by solving the following nonlinear constrained integer programming:

$$\begin{aligned} \min \quad & \sum_{h=1}^H |sl_{i_adj}^h - sl_{i_opt}^h| \\ \text{s.t.} \quad & sl_{ik}^h = sl_{ik}, \quad h \in [t_{ik}, t_{ik} + \Delta T_{ik}] \\ & sl_{ik}^h = 0, \quad h \notin [t_{ik}, t_{ik} + \Delta T_{ik}] \\ & [t_{ik}, t_{ik} + \Delta T_{ik}] \in [\alpha_{ik}, \beta_{ik}]; \sum_{h=t_{ik}}^{t_{ik} + \Delta T_{ik}} sl_{ik}^h = sq_{ik} \end{aligned}$$

- 3: Save the optimized t_{ik} ($k \in [1, 2, \dots, K_i]$), which will be adopted in shiftable load arrangement.

VI. CASE STUDIES

A. Basic data

In this section, we apply the proposed model in a MG. We employ MATLAB software to programme for solving the problem, and analyze the optimized results. In the MG, there are 6 residential buildings, and each of them is regared as a prosumer here. All of the prosumers have installed PV systems with capacity ranging from 50 to 400 kWp. The basic profiles of the prosumers are shown in TABLE I. For the convenience of study, each prosumer is assumed to have dozens or hundreds of shiftable load appliances, and the energy consumption characteristics of these appliances are collected from [24]. The shiftable loads' electricity proportion is nearly 20%. Based on the historical data collected from the real case buildings, the load and PV power for a typical winter day are obtained by the method introduced in [25], as shown in Fig.5.

TABLE I
THE PROFILES OF PROSUMERS IN THE MG

Name of the prosumers	Capacity of PV(kWp)	The maximum electric load (kW)	The maximum heat load (kW)
Prosumer 1	80	90.1	61.74
Prosumer 2	100	101.3	76.29
Prosumer 3	80	99.7	81.90
Prosumer 4	100	106.8	80.50
Prosumer 5	80	75.5	76.58
Prosumer 6	80	104.1	63.28

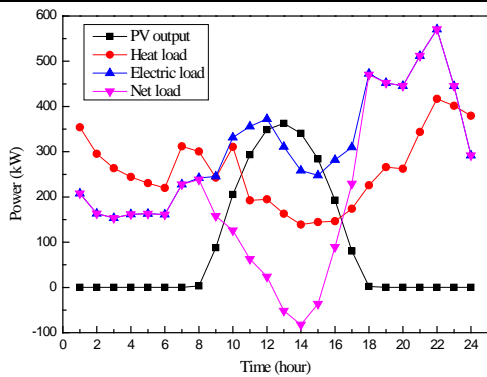


Fig. 5. Total power curves of all prosumers in a winter typical day

As shown in Fig. 5, the peak of the total electric load of all the prosumers is about 570kW at 22:00 PM, while the peak of

heat load is about 420kW at 22:00 PM as well. The maximum PV power output is about 360 kW at 13:00 PM. The PV output peak and the load peak are not synchronized. In this case, we set k_i equal to 100, and all prosumers take the same value. The related parameters in this case are shown in Table II.

TABLE II
THE RELATED PARAMETERS IN THE CASE

Subjects	Name of parameter	Value of parameter
MGO/Microturbine	Rated output electric power	500kW
	η_{chp}	0.4
	η_{loss}	0.05
	δ_{heat}	1.17
	p_{gas}	1.5 Yuan/m ³
	γ	0.15 Yuan/kWh (41.7 Yuan/GJ)
Prosumers	α	0.42 Yuan/kW
	$k_i, i \in N$	100

B. Results of MGO prices

The proposed model is applied to the MG, and the optimization iterative processes of MGO profit and prosumers' profits are shown in Fig. 6. We note that the convergence is reached after about 40 iterations. The changing tendency of the MGO profit is different from that of the prosumers' profits. The MGO profit gradually increases, while the prosumers' profits diminish with the increase of the iteration number.

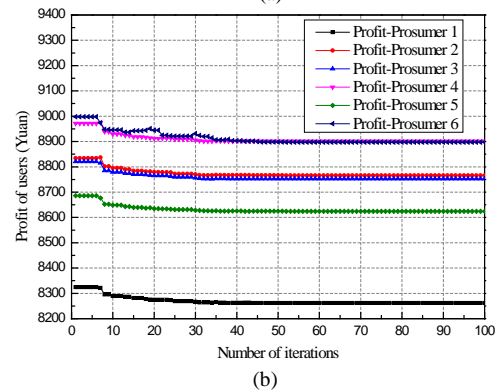
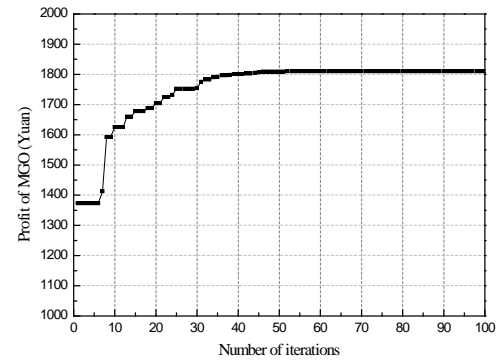


Fig. 6. The optimization iterative process: (a) profit of the MGO; (b) profits of the prosumers.

The power grid's TOU price curves in this case are plotted as dashed lines in Fig. 7. And the optimized results of MGO

selling prices are plotted as blue solid line, while MGO buying prices are plotted as red line in Fig. 7.

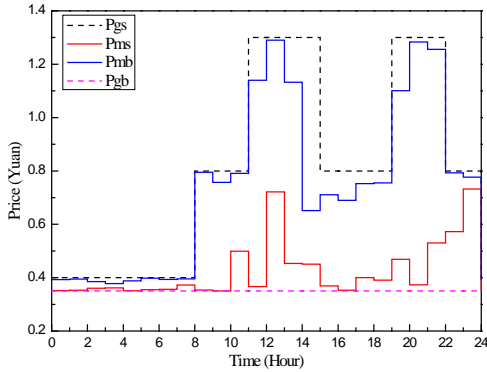


Fig. 7. The optimized results of MGO prices.

As shown in Fig. 7, MGO's selling prices are lower than the power grid's selling prices, and MGO's buying prices are higher than the power grid's buying prices. So the proposed model is more beneficial for the prosumers, compared with the situation that the prosumers trade with the power grid directly.

C. Results of shiftable loads and net loads

The original values and the results of prosumers' total shiftable loads from the proposed model are shown in Fig. 8. In the figure, the adjusted values are solved using **Algorithm 3** on the basis of the optimized values.

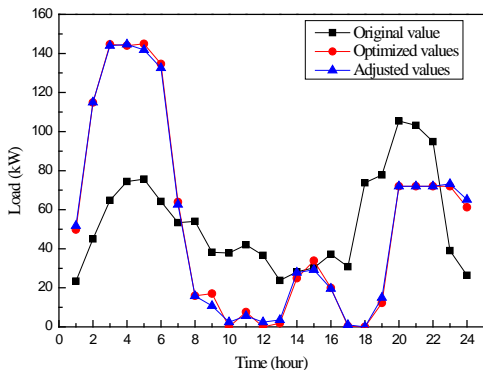


Fig. 8. Curves of the total shiftable loads of all prosumers.

As shown in Fig. 8, the shiftable load calculated by the proposed model presents a large peak around 4:00 AM, and two smaller peaks around 15:00 PM and 21:00 PM respectively. Compared with the original curve, the maximum value of the curve is shifted from 20:00 PM to 4:00 AM with the proposed model. The original minimum value around the midnight, is shifted to 10:00 AM~12:00 AM with the proposed model. Comparing Fig. 8 with Fig. 7, it is obvious that the peak regions of the total optimized shiftable load coincides with the valley position of the MGO prices. And when the MGO prices are higher, such as 11:00 AM ~15:00 PM and 19:00 PM ~22:00 PM, the shiftable loads are decreased as a whole with the proposed model. Moreover, we can find that the adjusted value curve is much close to the optimized value curve in Fig. 8.

D. Comparison with centralized optimization

As discussed in the Introduction, existing work mainly use the centralized method to design the EMS for MGs consist of CHP and PV prosumers. In order to compare the proposed

distributed method with the centralized method, we have transformed the scenario of the case study to a new scenario which can be solved by the centralized method. A generic centralized optimization only contains one centralized decision-maker that is responsible for optimizing all the variables involved in the model. In our centralized scenario, the only decision-maker is the MGO, who will determine all the variables, including MGO's prices and shiftable loads of prosumers. The optimization objective is to maximize the MGO's profit. Thus, the related information of PV prosumers (i.e., constraints of shiftable loads, and forecasting of load and PV power, etc.) should be provided to MGO. The results of net load curves and profits are shown in Fig. 9 and Fig. 10.

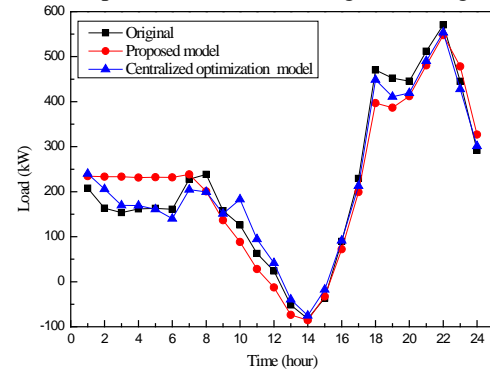


Fig. 9. Curves of the total net load with centralized optimization model and the proposed model.

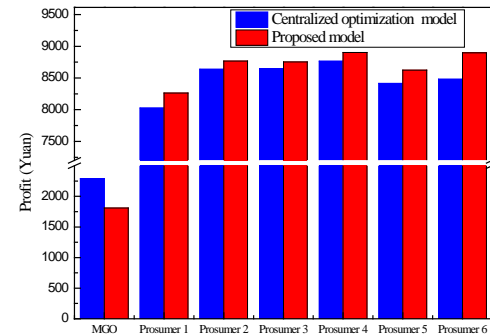


Fig. 10. Comparison of the profits with centralized optimization model.

As the roles of MGO and prosumers are different in these two methods, apparent distinctions appear in the results of net load curves and profits. We also found that the most obvious difference of the total net load appears at 1:00 am – 7:00 am.

In the scenario of centralized optimization, the only purpose is to maximize the profit of MGO, and the prosumers' load scheduling are decided by the MGO as well. As shown in Fig. 7, the differences between MGO's buying prices and selling prices (i.e., p_{mb} and p_{ms}) would be very small at 1:00 am – 7:00 am, and the selling prices are also the lowest in this period during the whole day. These are all negative for the MGO to enhance its daily profit by arranging the prosumers to increase power consumption during this time period.

While in the scenario of distributed optimization, the prosumers' load scheduling could be decided by themselves according to the MGO's prices. Unlike in the centralized method, the prosumer would increase power consumption at 1:00 am – 7:00 am in order to improve its profit, as the MGO's selling prices are the lowest in this period. It is obviously that the effectiveness of the centralized method is worse than the

proposed distributed method in term of optimizing net load profile of the MG.

As shown in Fig. 10, the profit of MGO is much higher (27%), while the profits of prosumers are all lower in the centralized scenario. Therefore, it is possible to increase the MGO profit while reduce the prosumers' profit adopting a centralized method. However, we can find that the proposed distributed method highlights the autonomy and independence of prosumers in decision-making, which is more close to the actual situation.

E. Sensitive analysis for the number of prosumers

We apply the model in cases with more prosumers in order to verify the applicability in larger residential MGs. The iterative process of MGO profit is shown in Fig. 11.

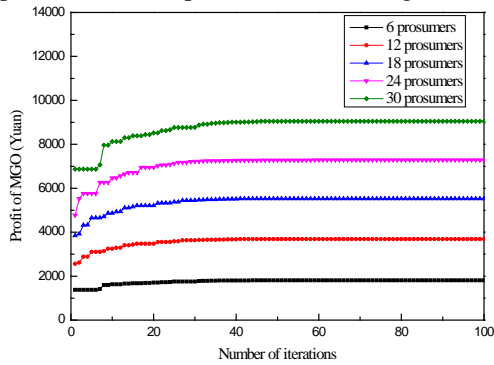


Fig. 11. The optimization iterative process of MGO profit with different n .

As shown in Fig. 11, the MGO profit with different prosumer numbers all converge to a stable state after 40 iterations. The result indicates that the model can also be applied to a large residential MG.

VII. CONCLUSION

In this paper, a dynamic pricing and energy management optimization model based on a Stackelberg game has been proposed for the joint operation of the CHP and prosumers in a MG. The prosumers have been modeled as the followers of the game who choose their strategies in response to the strategy of MGO, the leader of the game. It has been shown that there exists a unique Stackelberg equilibrium of the proposed game and heuristic algorithms based on DE has been proposed to reach the unique solution. The case studies have shown that the model can effectively determine the MGO's prices, and improve the load characteristics of the whole MG. The net load and profit differences between the centralized model and the proposed model have also been analyzed.

Considering the number of participated prosumers, the difference between the generated PV power curve and the forecasted curve may be large for the actual operation. In the future, there are possible two ways to solve this problem: 1) design a re-scheduling and re-pricing model according to the real-time errors; 2) as the prosumers are obligated to take own risks for their forecasting errors, design a punishment strategy for the prosumers' final electricity bill.

APPENDICES

A. The uniqueness of prosumers' optimal strategies

According to equation (31) and Fig. 3, We can imagine that there might be several situations of prosumer's profit profiles as shown in Fig. 12.

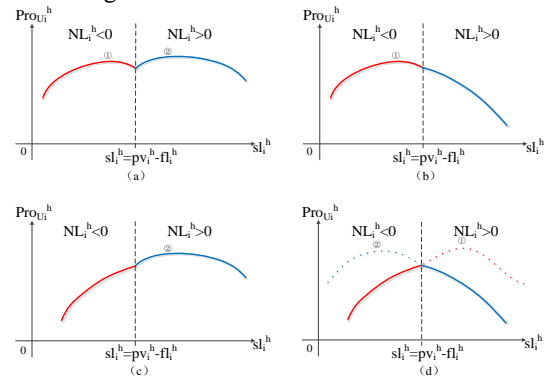


Fig. 12. Profiles of prosumer's profit that might appear.

When $NL_i^h < 0$, equation (31) can be rewritten as:

$$Pro_{U_i}^h = k_i \cdot \ln(1 + tl_i^h) - p_{mb}^h \cdot NL_i^h - fl_i^h \cdot \gamma + pv_i^h \cdot \alpha \quad (38)$$

Setting the derivative of (38) with respect to sl_i^h equal to zero,

$$\frac{\partial(Pro_{U_i}^h)}{\partial(sl_i^h)} = \frac{k_i}{1+fl_i^h+sl_i^h} - p_{mb}^h = 0, \quad (39)$$

we can get

$$sl_{i_0}^h = \frac{k_i}{p_{mb}^h} - fl_i^h - 1. \quad (40)$$

When $NL_i^h > 0$, equation (31) can be rewritten as:

$$Pro_{U_i}^h = k_i \cdot \ln(1 + tl_i^h) - p_{ms}^h \cdot NL_i^h - fl_i^h \cdot \gamma + pv_i^h \cdot \alpha \quad (41)$$

Similarly, setting the derivative of (41) with respect to sl_i^h equal to zero,

$$\frac{\partial(Pro_{U_i}^h)}{\partial(sl_i^h)} = \frac{k_i}{1+fl_i^h+sl_i^h} - p_{ms}^h = 0, \quad (42)$$

we can get

$$sl_{i_0}^h = \frac{k_i}{p_{ms}^h} - fl_i^h - 1. \quad (43)$$

Next, we will discuss the optimal solutions in different situations as described in Fig. 12.

a) In Fig. 12 (a), there are two maximum value points, located at $sl_{i_0}^h = \frac{k_i}{p_{mb}^h} - fl_i^h - 1$ and $sl_{i_0}^h = \frac{k_i}{p_{ms}^h} - fl_i^h - 1$ respectively. According to Fig. 12 (a), the former $sl_{i_0}^h$ is smaller than the latter, i.e., $\frac{k_i}{p_{mb}^h} - fl_i^h - 1 < \frac{k_i}{p_{ms}^h} - fl_i^h - 1$, then we can get

$$p_{mb}^h > \frac{k_i}{pv_i^h + 1} > p_{ms}^h. \quad (44)$$

Because p_{ms}^h should be larger than p_{mb}^h in reality, which is opposite to equation (44), so the situation in Fig. 12 (a) is impractical.

b) In Fig. 12 (b), the only maximum value points is located at $sl_{i_0}^h = \frac{k_i}{p_{mb}^h} - fl_i^h - 1$, which should be smaller than $pv_i^h - fl_i^h$, considering equation (23) as well, we can get

$$p_{ms}^h > p_{mb}^h > \frac{k_i}{pv_i^h + 1} \quad (45)$$

c) Similar to b), the only maximum value points in Fig. 12 (c) is located at $sl_{i_0}^h = \frac{k_i}{p_{ms}^h} - fl_i^h - 1$, and we can get

$$\frac{k_i}{pv_i^{h+1}} > p_{ms}^h > p_{mb}^h \quad (46)$$

d) In Fig. 12 (d), there are two maximum value points, located at $sl_{i,0}^h = \frac{k_i}{p_{mb}^h} - fl_i^h - 1$ and $sl_{i,0}^h = \frac{k_i}{p_{ms}^h} - fl_i^h - 1$ respectively. Clearly these two maximum points are both outside of the defined interval, but they will still satisfy $\frac{k_i}{p_{mb}^h} - fl_i^h - 1 > pv_i^h - fl_i^h > \frac{k_i}{p_{ms}^h} - fl_i^h - 1$, then we can get

$$p_{ms}^h > \frac{k_i}{pv_i^{h+1}} > p_{mb}^h. \quad (47)$$

And in this situation, the only maximum point in the defined interval is $sl_{i,0}^h = pv_i^h - fl_i^h$.

In conclusion, except the impractical situation in Fig. 12 (a), the prosumers always have the only optimal solution in the defined interval in situations shown in Fig. 12 (b) to Fig. 12 (d). The values of optimal solutions depend on the relationship between $\frac{k_i}{pv_i^{h+1}}$ and p_{ms}^h, p_{mb}^h . Each situation is related to one kind of relationship, which is defined in equation (45), (46), and (47) respectively.

B. The uniqueness of MGO's optimal strategy

For the MGO, there also exist two situations, i.e., $NL^h - ep_{chp}^h > 0$ and $NL^h - ep_{chp}^h < 0$. Due to space constraints, here we will just discuss the former situation.

It is assumed that the prosumers' amounts corresponding to three situations shown in Fig. 12 (b), Fig. 12 (c) and Fig. 12 (d) are x, y, z respectively. Then equation (25) can be rewritten as:

$$\begin{aligned} Pro_M^h = & -p_{gs}^h \cdot \left(\sum_{j=1}^y \left(\frac{k_j}{p_{ms}^h} - 1 - pv_j^h \right) + \sum_{i=1}^x \left(\frac{k_i}{p_{mb}^h} - 1 - pv_i^h \right) \right) \\ & + \sum_{j=1}^y p_{ms}^h \cdot \left(\frac{k_j}{p_{ms}^h} - 1 - pv_j^h \right) + \sum_{i=1}^x p_{mb}^h \cdot \left(\frac{k_i}{p_{mb}^h} - 1 - pv_i^h \right) \\ & + \gamma \cdot \sum_{i=1}^n hl_i^h - C_{CHP}^h \end{aligned} \quad (48)$$

The derivatives of (48) with respect to p_{ms}^h and p_{mb}^h are

$$\frac{\partial(Pro_M^h)}{\partial(p_{ms}^h)} = p_{gs}^h \cdot \sum_{j=1}^y \frac{k_j}{(p_{ms}^h)^2} + \sum_{j=1}^y (-1 - pv_j^h), \quad (49)$$

$$\frac{\partial(Pro_M^h)}{\partial(p_{mb}^h)} = p_{gs}^h \cdot \sum_{i=1}^x \frac{k_i}{(p_{mb}^h)^2} + \sum_{i=1}^x (-1 - pv_i^h). \quad (50)$$

Setting the above derivatives equal to zero, we can get $P_{m,0}(p_{ms,0}^h, p_{mb,0}^h)$, in which

$$p_{ms,0}^h = \sqrt{\frac{p_{gs}^h \cdot \sum_{j=1}^y k_j}{\sum_{j=1}^y (1 + pv_j^h)}}, p_{mb,0}^h = \sqrt{\frac{p_{gs}^h \cdot \sum_{i=1}^x k_i}{\sum_{i=1}^x (1 + pv_i^h)}}. \quad (51)$$

The Hessian matrix of Pro_M^h in equation (25) can be expressed as:

$$\begin{aligned} H(Pro_M^h) = & \begin{bmatrix} \frac{\partial^2 Pro_M^h}{\partial(p_{ms}^h)^2} & \frac{\partial^2 Pro_M^h}{\partial(p_{ms}^h)\partial(p_{mb}^h)} \\ \frac{\partial^2 Pro_M^h}{\partial(p_{mb}^h)\partial(p_{ms}^h)} & \frac{\partial^2 Pro_M^h}{\partial(p_{mb}^h)^2} \end{bmatrix} \\ = & \begin{bmatrix} -2p_{gs}^h \cdot \sum_{j=1}^y \frac{k_j}{(p_{ms}^h)^3} & 0 \\ 0 & -2p_{gs}^h \cdot \sum_{i=1}^x \frac{k_i}{(p_{mb}^h)^3} \end{bmatrix} \end{aligned} \quad (52)$$

Because determinant of the Hessian matrix $|H(Pro_M^h)| = 4p_{gs}^h \cdot p_{gs}^h \cdot \sum_{j=1}^y \frac{k_j}{(p_{ms}^h)^3} \cdot \sum_{i=1}^x \frac{k_i}{(p_{mb}^h)^3} > 0$, and $\frac{\partial^2 Pro_M^h}{\partial(p_{ms}^h)^2} <$

0 , so $P_{m,0}(p_{ms,0}^h, p_{mb,0}^h)$ is the only maximum value point.

REFERENCES

- [1] W. Su, J. Wang, and J. Roh, "Stochastic energy scheduling in microgrids with intermittent renewable energy resources," *IEEE Trans. Smart Grid*, vol. 5, no. 4, pp. 1876-1883, 2014.
- [2] D. Wang, S. Ge, H. Jia, C. Wang, Y. Zhou, N. Lu, and X. Kong, "A demand response and battery storage coordination algorithm for providing microgrid tie-line smoothing services," *IEEE Trans. Sust. Energ.*, vol. 5, no. 2, pp. 476-486, 2014.
- [3] N. Liu, Q. Chen, X. Lu, J. Liu, and J. Zhang, "A Charging Strategy for PV-Based Battery Switch Stations Considering Service Availability and Self-Consumption of PV Energy," *IEEE Trans. Ind. Electron.*, vol. 62, no. 8, pp. 4878-4889, 2015.
- [4] B. Zhao, X. Zhang, J. Chen, C. Wang, and L. Guo, "Operation optimization of standalone microgrids considering lifetime characteristics of battery energy storage system," *IEEE Trans. Sust. Energ.*, vol. 4, no. 4, pp. 934-943, 2013.
- [5] R. Palma-Behnke, C. Benavides, F. Lanas, B. Severino, L. Reyes, J. Llanos, and D. Saez, "A Microgrid Energy Management System Based on the Rolling Horizon Strategy," *IEEE Trans. Smart Grid*, vol. 4, no. 2, pp. 996-1006, 2013.
- [6] C. Milan, M. Stadler, G. Cardoso, and S. Mashayekh, "Modeling of non-linear CHP efficiency curves in distributed energy systems," *Appl. Energy* vol. 148, pp. 334-347, 2015.
- [7] A. Hawkes, and M. Leach, "Cost-effective operating strategy for residential micro-combined heat and power," *Energy*, vol. 32, no. 5, pp. 711-723, 2007.
- [8] P. Palensky, and D. Dietrich, "Demand Side Management: Demand Response, Intelligent Energy Systems, and Smart Loads," *IEEE Trans. Ind. Inf.*, vol. 7, no. 3, pp. 381-388, 2011.
- [9] D. E. Olivares, Can, x, C. A. izares, and M. Kazerani, "A Centralized Energy Management System for Isolated Microgrids," *IEEE Trans. Smart Grid*, vol. 5, no. 4, pp. 1864-1875, 2014.
- [10] H. Kanchev, D. Lu, F. Colas, V. Lazarov, and B. Francois, "Energy management and operational planning of a microgrid with a PV-based active generator for smart grid applications," *IEEE Trans. Ind. Electron.*, vol. 58, no. 10, pp. 4583-4592, 2011.
- [11] M. Motevasel, A. R. Seifi, and T. Niknam, "Multi-objective energy management of CHP (combined heat and power)-based micro-grid," *Energy*, vol. 51, pp. 123-136, 2013.
- [12] Z. Wang, K. Yang, and X. Wang, "Privacy-preserving energy scheduling in microgrid systems," *IEEE Trans. Smart Grid*, vol. 4, no. 4, pp. 1810-1820, 2013.
- [13] W. Saad, Z. Han, H. V. Poor, and T. Basar, "Game-theoretic methods for the smart grid: An overview of microgrid systems, demand-side management, and smart grid communications," *IEEE Signal Processing Mag.*, vol. 29, no. 5, pp. 86-105, 2012.
- [14] D. Gregoratti, and J. Matamoros, "Distributed energy trading: the multiple-microgrid case," *IEEE Trans. Ind. Electron.*, vol. 62, no. 4, pp. 2551-2559, 2015.
- [15] E. Dall'Anese, H. Zhu, and G. Giannakis, "Distributed optimal power flow for smart microgrids," *IEEE Trans. Smart Grid*, vol. 4, no. 3, pp. 1464-1475, 2013.
- [16] C. Marnay, G. Venkataramanan, M. Stadler, A. S. Siddiqui, R. Firestone, and B. Chandran, "Optimal technology selection and operation of commercial-building microgrids," *IEEE Trans. Power Syst.*, vol. 23, no. 3, pp. 975-982, 2008.
- [17] J. Aghaei, and M.-I. Alizadeh, "Multi-objective self-scheduling of CHP (combined heat and power)-based microgrids considering demand response programs and ESSs (energy storage systems)," *Energy*, 2013, pp. 1044-1054.
- [18] W. Gu, Z. Wu, and X. Yuan, "Microgrid economic optimal operation of the combined heat and power system with renewable energy," in *Proc. IEEE Power Energy Soc. Gen. Meet.*, 2010, pp. 1-6.
- [19] W. Tushar, B. Chai, C. Yuen, D. B. Smith, K. L. Wood, Z. Yang, and H. V. Poor, "Three-party energy management with distributed energy resources in smart grid," *IEEE Trans. Ind. Electron.*, vol. 62, no. 4, pp. 2487-2498, 2015.
- [20] M. Yu, and S. H. Hong, "A Real-Time Demand-Response Algorithm for Smart Grids: A Stackelberg Game Approach," *IEEE Trans. Smart Grid*, vol. 7, no. 2, pp. 879-888, 2016.

- [21] J. Chen, X. Yang, L. Zhu, and M. Zhang, "Genetic algorithm based economic operation optimization of a combined heat and power microgrid," *Power Sys. Prot. Control.*, vol. 41, no. 8, pp. 7-15, 2013 (in Chinese).
- [22] S. Boyd, and L. Vandenberghe, *Convex optimization*: Cambridge university press, 2004.
- [23] R. Storn, and K. Price, "Differential evolution—a simple and efficient heuristic for global optimization over continuous spaces," *J. Global Optim.*, vol. 11, no. 4, pp. 341-359, 1997.
- [24] C. Li, X. Yu, W. Yu, G. Chen, and J. Wang, "Efficient Computation for Sparse Load Shifting in Demand Side Management," *IEEE Trans. Smart Grid*, vol. PP, no. 99, pp. 1-12, 2016.
- [25] N. Liu, Q. Tang, J. Zhang, W. Fan, and J. Liu, "A hybrid forecasting model with parameter optimization for short-term load forecasting of micro-grids," *Appl. Energy* vol. 129, pp. 336-345, 2014.



Li Ma received the B.S. and M.S. degrees in electric engineering from North China Electric Power University, Beijing, China, in 2008 and 2011, respectively.

Currently, she is pursuing the Ph.D. degree in the School of Electrical and Electronic Engineering of North China Electric Power University, Beijing, China. She has been also with the China Electric Power Research Institute as an Engineer since 2011.

Her research interests include smart grid, game theory, and urban distribution network planning.



Nian Liu (S'06-M'11) received the B.S. and M.S. degrees in electric engineering from Xiangtan University, Hunan, China, in 2003 and 2006, respectively, and the Ph.D. degree in electrical engineering from North China Electric Power University, Beijing, China, in 2009.

Currently, he is an Associate Professor in the School of Electrical and Electronic Engineering of North China Electric Power University, Beijing, China. He is also a Visiting Research Fellow with RMIT University, Melbourne, Australia.

His research interests include demand side energy management, microgrids, electric vehicles, and cyber security of smart grid.



Jianhua Zhang (M'04) was born in Beijing, China, in 1952. He received the M.S. degree in electrical engineering from North China Electric Power University, Beijing, China, in 1984.

He was a Visiting Scholar with the Queen's University, Belfast, U.K., from 1991 to 1992, and was a Multimedia Engineer of Electric Power Training with CORYS T.E.S.S., France, from 1997 to 1998. Currently, he is a Professor and Head of the Transmission and Distribution Research Institute, North China Electric Power University, Beijing. He

is also the Consultant Expert of National "973" Planning of the Ministry of Science and Technology. His research interests are in power system security assessment, operation and planning, and micro-grid.

Prof. Zhang is an IET Fellow and a member of several technical committees.



Wayes Tushar (S'06, M'13) received the B.Sc. degree in Electrical and Electronic Engineering from Bangladesh University of Engineering and Technology (BUET), Bangladesh in 2007 and the Ph.D. degree in Engineering from the Australian National University (ANU), Australia in 2013.

Currently, he is Research Scientist at the SUTD-MIT International Design Center (IDC) in Singapore University of Technology and Design (SUTD), Singapore. Prior joining SUTD, he was with National ICT Australia (NICTA) as a visiting

researcher (January 2013 to June 2013) and was a visiting student research collaborator at Princeton University, USA (Summer 2011). He is the recipient of two best paper awards in IEEE International Conference on

Communications (ICC), 2013 and Australian Communications Theory Workshop (AusCTW), 2012.

His research interests include smart grid and game theory.



Chau Yuen (S'02-M'08-SM'12) received the B.Eng. and Ph.D. degrees from Nanyang Technological University, Singapore, in 2000 and 2004, respectively. He was a Post-Doctoral Fellow with Lucent Technologies Bell Laboratories, Murray Hill, in 2005. He was also a Visiting Assistant Professor with Hong Kong Polytechnic University in 2008. From 2006 to 2010, he was with the Institute for Infocomm Research, Singapore, as a Senior Research Engineer.

He has been with the Singapore University of Technology and Design as an Assistant Professor since 2010. In 2012, he received the IEEE Asia-Pacific Outstanding Young Researcher Award. He currently serves as an Associate Editor of the IEEE TRANSACTIONS ON VEHICULAR TECHNOLOGY.